Spreading laws for diffusion in a low-Reynolds-number channel

By J. Jiménez†,

1. Introduction

It was shown by del Álamo *et al.* (2004) and by Jiménez, del Álamo & Flores (2004) that the spectral energy densities of the streamwise velocity fluctuations in turbulent channels contain relatively-narrow ridges at long wavelengths, scaling as $\lambda_z \sim \lambda_x^{1/3}$ in the viscous and buffer sublayers, and as $\lambda_z \sim \lambda_x^{1/2}$ in the logarithmic region. The wavelengths λ_x and λ_z in those expressions can be interpreted as characteristic streamwise and spanwise dimensions of individual velocity structures, and it was argued by those authors that those two laws could be explained by the spreading of wakes left in the mean velocity profile by compact wall-normal-velocity structures.

It has indeed often been noted that, for long streamwise structures, the equations for the streamwise and for the flow-normal velocity components approximately decouple, and that the former can be approximated as a passive species advected by the latter (Orlandi & Jiménez 1994). In a turbulent flow this advection can approximately be represented as a turbulent diffusion. It was shown by del Álamo *et al.* (2004) that reasonable assumptions on the advection velocity of the generating structures and on the effective eddy viscosity yield spreading rates which agree quantitatively with the spectral square-root behavior observed in the logarithmic layer. It was also noted by Jiménez, del Álamo & Flores (2004) that the cube-root law is the similarity solution for diffusion in a uniform shear under the effect of a constant diffusion coefficient, both of which are reasonable assumptions near the wall. Finally, the physical structure of the wakes in the logarithmic region was isolated by means of conditional statistics in del Álamo *et al.* (2005), and supporting evidence for wakes in the buffer layer was provided by Jiménez, del Álamo & Flores (2004).

On the other hand, the coexistence of two different power laws remains to our knowledge undocumented in other flows, and would benefit from a quantitative theoretical explanation in at least one case. Since diffusion in turbulent channels, which requires delicate modelling of the effective diffusion coefficients at various flow locations, remains complicated, we will present here the analysis of the spanwise spreading of a mixing layer in a laminar low-Reynolds flow, and we will show that it already contains the two power-law regimes.

That shear influences diffusion is well known. Taylor (1953, 1954) showed in two classic papers that the effective diffusion coefficient of a solute is strongly modified when the mixing occurs in a shear flow. His analysis deals with the experimentally-important case in which the solute is injected as a plug filling a tube, and the diffusion is nominally streamwise. It therefore competes with the advection by the sheared streamwise velocity, which generates a wall-normal concentration gradient that is responsible for the enhanced diffusion. Recently Baroud *et al.* (2002) implemented a different experimental

† School of Aeronautics, Universidad Politécnica, 28040 Madrid, Spain

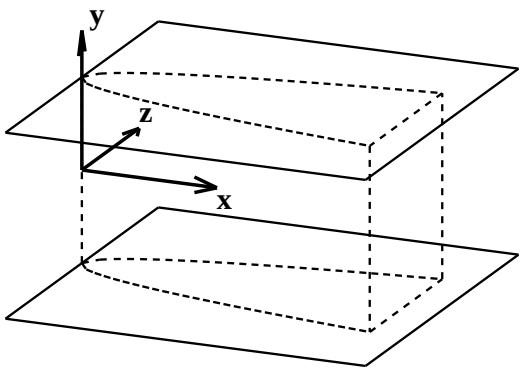

FIGURE 1. Problem geometry

configuration in which the diffusion happens in a narrow channel in which two streams of different solute concentration are injected side by side in the spanwise direction. The conditions are such that, although the Reynolds number of the flow is low enough for the mean velocity profile to be considered parabolic, the Péclét number of the solute is large, and the lateral diffusion occurs slowly. Since the longitudinal evolution of the mixing layer is then also slow, its interaction with the streamwise shear is weaker than in the plug case, but its growth is still modified. It is indeed clear that, were it not for the wall-normal diffusion, the mixing layer would grow at different rates at different wall distances, corresponding to the different local velocities. In this paper we analyze the diffusion of a solute under those conditions in enough detail to allow the experimental arrangement to be used in the determination of molecular diffusion coefficients. As discussed above a secondary motivation is to document the dependence on the wall distance of the spreading exponents, and to compare it with the ones observed in wall turbulence.

2. Basic scaling

Consider a channel between two parallel plates located at $y = \pm h$, and denote by $\widetilde{x}$ and $\widetilde{z}$ the streamwise and spanwise coordinates (see figure 1). Normalize the parabolic velocity profile U with its maximum, and the coordinates with h, so that $U = 1 - y^2$. Two streams with different concentrations of a passive scalar c are initially at $\widetilde{z} > 0$ and $\widetilde{z} < 0$, and come together at $\widetilde{x} = 0$. The diffusion equation for c is

$$Pe\,(1 - y^2)\partial_x c = \partial_{\widetilde{x}\widetilde{x}} c + \partial_{yy} c + \partial_{\widetilde{z}\widetilde{z}} c, \tag{2.1}$$

where $Pe = U_c h/\kappa \gg 1$, and κ is the diffusivity of c. We will assume that there is no diffusion flux into the walls, so that

$$\partial_y c = 0, \text{ at } y = \pm 1, \tag{2.2}$$

and that the mixing takes place between

$$c = \pm 1/2, \text{ at } \widetilde{z} = \pm\infty. \tag{2.3}$$

Note that, since the problem is linear and homogeneous in $\widetilde{z}$, the same analysis can applied to the spreading of an initially-thin contaminant layer by differentiating everything with respect to $\widetilde{z}$.

As long as $\widetilde{x} \gg 1$ the streamwise diffusion term is negligible with respect to the other

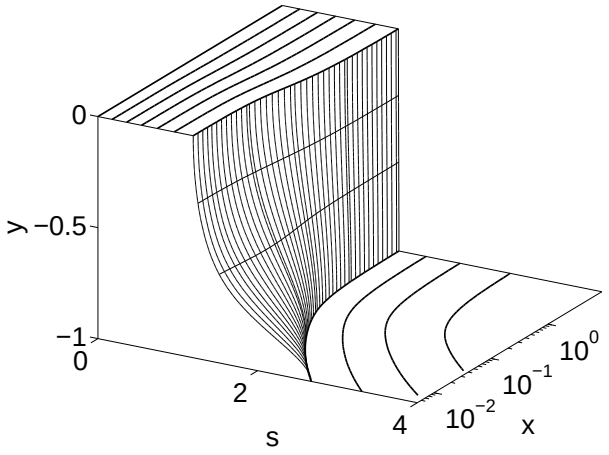

FIGURE 2. Numerical solution of (2.4), for $s > 0$ and $y < 0$. The wall is at the bottom, and the channel center at the top. The flow is from bottom–left to top–right. The isosurface represented is $c = 0.3$. The isolines on the top plane are $c = 0.05(0.05)0.3$, and those at the bottom plane are $c = 0.3(0.05)0.45$.

two directions, and can be neglected. The spreading of the mixing layer involves the balance of the streamwise advection with the spanwise diffusion, which have to be of the same order. If $\widetilde{x} = O(L)$, the spanwise scale then has to be $\widetilde{z} = O(L/Pe)^{1/2}$. There is a natural scaling, $L = Pe$, in which the three remaining terms of (2.1) are of comparable magnitude. Defining stretched coordinates $x = \widetilde{x}/Pe$ and $z = \widetilde{z}/Pe^{1/2}$, we get

$$(1 - y^2)\partial_x c = \partial_{yy} c + \partial_{zz} c + O(Pe^{-2}). \tag{2.4}$$

The leading order of this equation is parameter-free, and can be integrated numerically. The solution is symmetric with respect to $y = 0$, and antisymmetric with respect to $z = 0$, and is shown in figure 2 as a function of the scaled x, of y, and of the usual similarity variable for two-dimensional diffusion problems

$$s = z/x^{1/2}. \tag{2.5}$$

It has been computed using a second-order Crank-Nicholson marching code, using 200 grid points in y, and between 200 and 800 points in z, depending on the distance to the origin. The step in x was refined to insure grid independence in the critical region of small x. The solution in the figure corresponds to the overlap of three different computations at three different x-ranges, and the lack of discontinuities between the ranges was used as a criterion for numerical convergence.

At the central plane the solution follows fairly well the square-root law, but near the wall it spreads faster, specially at the early stages of the mixing. Even at the central plane there is a transition in the growth rate around $x = 1$. To understand that behavior we consider next the two limits in which x is either much smaller or much larger than one.

3. The near limit, $\widetilde{x} \ll Pe$

This is the relevant experimental case when $Pe \gg 1$, because further downstream the mixing layer grows enough to interfere with the lateral walls of the apparatus. When

$x \ll 1$, the longitudinal transport and the transverse diffusion are the dominant terms in (2.4), and it is natural to attempt an expansion of the form

$$c = c_{n,0} + x c_{n,1} + \dots, \tag{3.1}$$

where the coefficient are functions of y and of s. They satisfy

$$\partial_{ss} c_{n,k} + (1-y^2)\left(\frac{s}{2}\partial_s c_{n,k} - k c_{n,k}\right) = -\partial_{yy} c_{n,k-1}, \tag{3.2}$$

which is a well-ordered hierarchy in which y appears only as a parameter. In the leading-order equation for $c_{n,0}$ the right-hand side vanishes, and the solution can be written immediately as

$$c_{n,0} = \frac{1}{2}\mathrm{erf}\,(Z/2), \tag{3.3}$$

where

$$Z = s(1-y^2)^{1/2}. \tag{3.4}$$

Equation (3.3) satisfies the boundary conditions for c at $z \to \pm\infty$, but not the zero-flux conditions (2.2) at the walls.

Consider the neighborhood of the lower wall, and define the distance to the wall as $y' = y + 1$. When $y' \ll 1$ the velocity is $U \approx 2y'$, and $c_{n,0}$ behaves as $y'^{1/2}$. In this region the width of the mixing layer given by (3.3) is $z = O([x/y']^{1/2})$, and there is a boundary layer of thickness $y' = O(x^{1/3})$ in which the wall-normal diffusion cannot be neglected. The three terms in (3.2) are then of the same order, and there are new similarity variables

$$\eta = y'/x^{1/3}, \tag{3.5}$$

and

$$\zeta = z/x^{1/3}, \tag{3.6}$$

in terms of which (3.2) becomes

$$\partial_{\eta\eta} c + \partial_{\zeta\zeta} c + \frac{2}{3}\eta(\eta\partial_\eta c + \zeta\partial_\zeta c) = O(x^{1/3}). \tag{3.7}$$

The error term in the right-hand side is due primarily to the expansion of U near the wall in terms of η. The concentration c must satisfy (2.2) at $\eta = 0$, and (2.3) at $\zeta = \pm\infty$. When $\eta \gg 1$, it also has to match the $y \ll 1$ limit of the outer solution (3.3),

$$c_{n,0} \approx \frac{1}{2}\mathrm{erf}\,[\zeta(\eta/2)^{1/2}]. \tag{3.8}$$

This is a parameter-free elliptic problem that can be solved numerically. Its solution, c_{BL}, is antisymmetric with respect to $\zeta = 0$, and is shown graphically in figure 3(a). It has been obtained in the domain $\zeta = (0, 8)$ and $\eta = (0, 6)$, using a straightforward second-order finite-difference code with a grid of 200×250 points. It tends to (3.8) away from the wall, but it does not become infinitely wide in ζ at the wall.

Note that the higher-order terms of the expansion for c_n become increasing singular near the wall. While the only singularity of $c_{n,0}$ comes from the similarity variable Z, the next term

$$c_{n,1} = -\frac{Z(3+3y^2+y^2Z^2)}{12\sqrt{\pi}(1-y^2)^3}\mathrm{e}^{-Z^2/4}, \tag{3.9}$$

has an extra factor factor y'^{-3}. It is easy to show that $c_{n,k}x^k$ behaves near the wall as $(x/y'^3)^k = \eta^{-3k}$. Since Z is also approximately $\zeta\eta^{1/2}$ in that limit, it follows that the

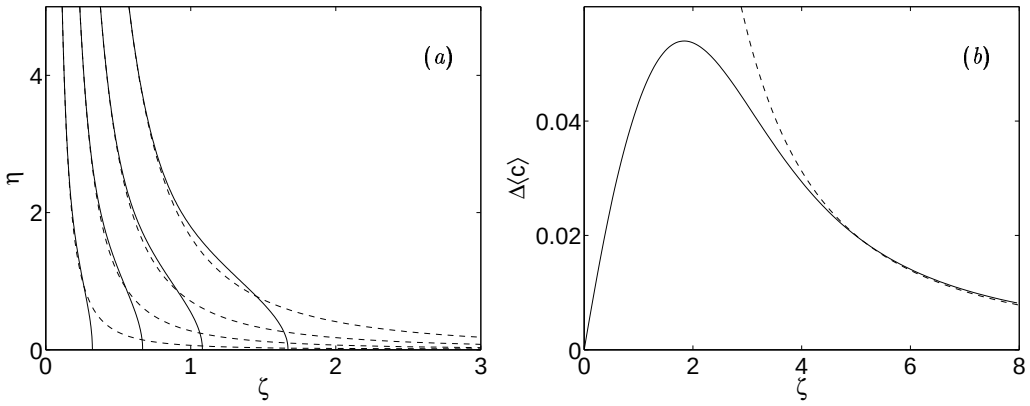

FIGURE 3. (*a*) Similarity solution for the boundary layer near the lower wall. ——— , similarity solution; ---- , outer solution (3.8). The contours are $c_{BL} = 0.1(0.1)0.4$. (*b*) Correction to the vertically-integrated concentration due to the boundary layer. ——— , $\langle c_{BL} - c_n \rangle$; ---- , large-$\zeta$ limit, $0.5/\zeta^2$.

inner limit of the outer solution is a function of ζ and η which has contributions from all the orders in the expansion (3.3). It is however clear from the previous discussion that the contributions to this function of the higher-order terms decay quickly as η increases, and that the boundary-layer solution can be matched safely to $c_{n,0}$ as long as the matching is done far enough. On the other hand, this is a problem in which the only way to avoid singularities in the higher-order terms is to use in the right-hand side of (3.2) the composite solutions formed by the lower-order boundary-layer and outer solutions, instead of just by the outer ones (Van Dyke 1964). This has no effect in the outer region, where the inner and outer solution coincide but, within the boundary layer where $\partial_{yy} c_{BL} = O(x^{-2/3})$, the correction $x c_1$ is $O(x^{1/3})$. This was already suggested by (3.7).

What is often measured in experiments is the vertically-integrated concentration

$$\langle c \rangle = \frac{1}{2} \int_{-1}^{1} c \, \mathrm{d}y. \tag{3.10}$$

It can be written in the present case as

$$\langle c \rangle \approx \langle c_{n,0} \rangle + x^{1/3} \langle \Delta c \rangle = \frac{\sqrt{\pi}}{8} s \exp(-s^2/8) \left[\mathrm{I}_0(s^2/8) + \mathrm{I}_1(s^2/8) \right] + x^{1/3} \langle \Delta c \rangle, \tag{3.11}$$

where I_0 and I_1 are Bessel functions. The correction $\langle \Delta c \rangle$ due to the boundary layers is

$$\langle \Delta c \rangle(\zeta) = \int_0^\infty (c_{BL} - c_{n,0}) \, \mathrm{d}\eta, \tag{3.12}$$

and is given in figure 3(*b*). For $\zeta \gg 1$ the solution c_{BL} is everywhere close to its asymptotic value 1/2, and (3.12) is mostly due to the integral of c_n, which can be evaluated exactly. That limit, $\langle \Delta c \rangle \approx 1/2\zeta^2$, is included in figure 3(*b*) for comparison.

Because $\langle c_n \rangle(s)$ and $\langle \Delta c \rangle(\zeta)$ depend differently on x it is impossible to express the composite solution in terms of a single similarity variable but, since (3.11) and (3.12) only hold in the limit $x \ll 1$, it is usually possible to write asymptotically valid expressions

for most quantities. Consider for example the 'slope' thickness defined by

$$\delta_s = \frac{c_\infty - c_{-\infty}}{\langle c \rangle'_{\widetilde{z}}}, \tag{3.13}$$

where $c'_{\widetilde{z}}$ stands for $\partial_{\widetilde{z}} c$ at $\widetilde{z} = 0$. Using the expressions above,

$$\delta_s^{-1} = \langle c_n \rangle'_s x^{-1/2} + \langle \Delta c \rangle'_\zeta \approx \frac{\sqrt{\pi}}{8} x^{-1/2} + 0.0551, \tag{3.14}$$

where $\langle c_n \rangle'_s$ follows from (3.11), and $\langle \Delta c \rangle'_\zeta$ has been estimated numerically from figure 3(b). Similar expressions can be obtained for other product thicknesses.

4. The limit $\widetilde{x} \gg Pe$

When $x \gg 1$, the mixing layer becomes much wider than h, and the dominant diffusion term is the one normal to the wall. We then look for expansions of the form,

$$c = c_{f,0} + x^{-1} c_{f,1} + \dots, \tag{4.1}$$

where the coefficients are again functions of s and y, and satisfy,

$$\partial_{yy} c_{f,k+1} = -\partial_{ss} c_{f,k} - (1 - y^2) \left(\frac{s}{2} \partial_s c_{f,k} + k c_{f,k} \right). \tag{4.2}$$

To leading order $\partial_{yy} c_{f,0} = 0$ and, from the boundary conditions (2.2), it follows that $c_{f,0}$ is only a function of s. To obtain it we must go to the next order, where

$$\partial_{yy} c_{f,1} = -(1 - y^2) \frac{s}{2} \partial_s c_{f,0} - \partial_{ss} c_{f,0}. \tag{4.3}$$

The correction $c_{f,1}$ also has to satisfy the Neumann conditions (2.2) at $y = \pm 1$, and it follows from the integration of (4.3) between the two walls that this is only possible if

$$\langle (1 - y^2) \rangle \frac{s}{2} \partial_s c_{f,0} + \partial_{ss} c_{f,0} = \frac{s}{3} \partial_s c_{f,0} + \partial_{ss} c_{f,0} = 0, \tag{4.4}$$

from where we write immediately

$$c_0 = \langle c_0 \rangle = \frac{1}{2} \mathrm{erf}\, (s/\sqrt{6}). \tag{4.5}$$

Note that the similarity variable in (4.5) is the same as the one for $\langle c_n \rangle$ in the previous section, but that the spreading rate is different. The first-order correction $c_{f,1}$ can be obtained by integrating (4.3) with respect to y, and contains an unknown additive function of s that has to satisfy a diffusion equation similar to (4.4), but the solution is now uniformly valid across the channel, and the correction is everywhere $O(x^{-1})$. To leading order, the mixing layer thickness is

$$\delta_s = (6\pi x)^{1/2}. \tag{4.6}$$

In figure 4(a) the evolution of the slope thickness obtained from the numerical solution of (2.4) is compared with the asymptotic expressions (3.14) and (4.6). The approximation is much better in the downstream case than in the one near the origin, in agreement with the different orders of the corrections which have been neglected, but the solution deviates little in general from a square-root growth law.

Note that we could have written the similarity variable s in these formulas with an arbitrary shift in the origin of x, since the approximation in this section does not hold

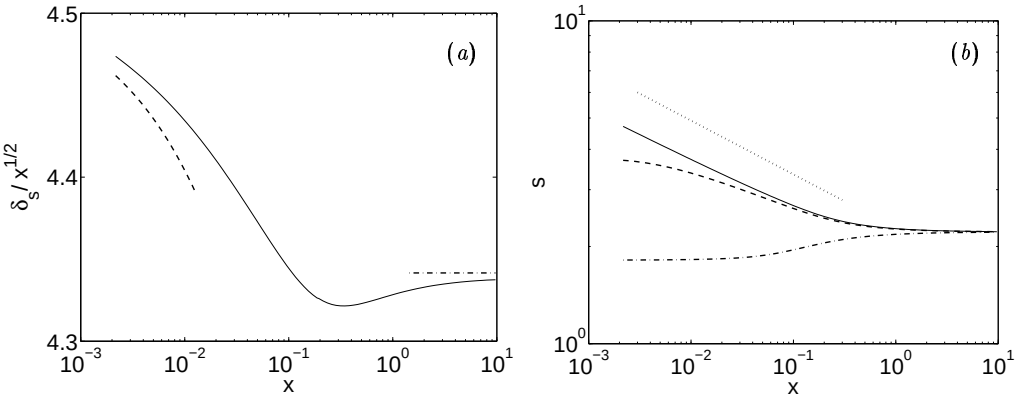

FIGURE 4. (*a*) Slope thickness of the mixing layer, scaled with $x^{1/2}$. ——— , numerical result; - - - - , small-x limit (3.14); —·— , large-x limit (4.6). (*b*) Lateral position of the isosurface $c = 0.4$, scaled with $x^{1/2}$, for different wall distances. ——— , $y' = 0.01$; - - - - , $y' = 0.15$; —·— , central plane. $y' = 1$. The dotted line corresponds to $z \sim x^{1/3}$.

at the physical origin of the mixing region. Any shift in the virtual origin can however be expected to be at most $x_0 = O(1)$, and would only appear in a large-x expansion as a term of $O(x^{-1})$.

The growth of the mixing layer at different distances from the wall is summarized in figure 4(*b*), which is compiled from the numerical results. The square-root growth appears as a constant in this plot, and it is the one followed by the layer in the central plane. The two different constants at small and large downstream locations correspond to the two outer solutions (3.8) and (4.5). Near the wall the layer follows initially the $x^{1/3}$ growth law, and only joins the square-root behavior when the mixing layer becomes vertically uniform farther downstream. The behavior of the intermediate location at $y' = 0.15$ is interesting. That wall distance is initially within the outer core of the channel, and follows approximately the square-root law. It then changes to an $x^{1/3}$ behavior as it is swallowed by the growth of the wall boundary layer, and it only returns to $x^{1/2}$ in the downstream limit in which the layer uniformizes.

5. Conclusions

We have shown that the spreading of a spanwise discontinuity of a passive scalar in a laminar channel is modified by the wall-normal diffusion due to the variation of the advection velocity with the distance to the wall. Because the spreading is orthogonal to the shear, this effect is weaker than in the case of longitudinal diffusion in tubes, but it has several experimentally-relevant effects. First, the spreading in the central plane is always approximately like $\widetilde{x}^{1/2}$, but the reasons are different near the origin and far from it, and the multiplicative constants change accordingly. Near the origin the wall-normal diffusion is negligible in this central region, but it becomes dominant far downstream, where the layer is much wider than the channel thickness. The layer then becomes uniform in the wall-normal direction, and behaves as if the advection velocity were constant and equal to the bulk velocity.

Near the origin the wall-normal diffusion is only important in boundary layers that develop near each wall. They have widths and heights of the order of $(\widetilde{x}/Pe)^{1/3}$, and they account for corrections of that order to the square-root behavior of the vertically-

integrated scalar profiles. The transition between the two regimes occurs at $\widetilde{x}/h \approx Pe$, when the wall layers fill the whole channel. We have given numerical results which can be used to interpret experiments.

We have noted that similar spreading laws are found in the growth of the structures of the streamwise velocity of turbulent channels. The effect of the wall-normal shear should also be their origin in that case, but there are extra complications connected with the variation of the eddy viscosity with the wall distance. That case will be the subject of a future study.

This work was supported in part by CICYT, under grant BPI2003-03434, and also the Department of Energy under the ASC program. I am grateful to S. Lele for his careful critique of an early version of this manuscript.

REFERENCES

DEL ÁLAMO, J.C., JIMÉNEZ, J., ZANDONADE, P. & MOSER, R.D. 2004 Scaling of the energy spectra of turbulent channels, *J. Fluid Mech.* **500**, 135–144.

DEL ÁLAMO, J.C., JIMÉNEZ, J., ZANDONADE, P. AND MOSER, R.D. 2005 Attached and detached vortex clusters in the logarithmic region, submitted *J. Fluid Mech.*

BAROUD, C.N., OKKELS, F., MÉNÉTRIER & TABELING, P. 2002 Reaction-diffusion dynamics: Confrontation between theory and experiment in a microfluidic reactor. *Phys. Rev.* E **67**, 060104-1.

JIMÉNEZ, J., DEL ÁLAMO, J.C. & FLORES, O. 2004 The large-scale dynamics of near-wall turbulence, *J. Fluid Mech.* **505**, 179–199.

ORLANDI, P. AND JIMÉNEZ, J. 1994 On the generation of turbulent wall friction, *Phys. Fluids* **6**, 634-641.

TAYLOR, G.I. 1953 Dispersion of soluble matter in solvent flowing slowly through a tube. *Proc. Roy. Soc. London* A **219**, 186–203.

TAYLOR, G.I. 1954 Conditions under which a solute in a stream of solvent can be used to measure molecular diffusion. *Proc. Roy. Soc. London* A **225**, 473–477.

VAN DYKE, M. 1964 *Perturbation methods in fluid mechanics*, Associated Press, 93–97.